

Critical Exponent of Chaotic Transients in Nonlinear Dynamical Systems

Celso Grebogi,^(a) Edward Ott,^{(a),(b)} and James A. Yorke^(c)

University of Maryland, College Park, Maryland 20742

(Received 28 April 1986)

The average lifetime of a chaotic transient versus a system parameter is studied for the case wherein a chaotic attractor is converted into a chaotic transient upon collision with its basin boundary (a crisis). Typically the average lifetime T depends upon the system parameter p via $T \sim |p - p_c|^{-\gamma}$, where p_c denotes the value of p at the crisis and we call γ the critical exponent of the chaotic transient. A theory determining γ for two-dimensional maps is developed and compared with numerical experiments. The theory also applies to critical behavior at interior crises.

PACS numbers: 05.45.+b

In dissipative dynamical systems it is common to see the destruction of a chaotic attractor as a parameter varies (a boundary crisis¹). As the parameter (call it p) is raised, the distance between the chaotic attractor and its basin boundary decreases until, at a critical value $p = p_c$, the attractor and its basin boundary touch (the crisis). For $p > p_c$ the chaotic attractor no longer exists, but is replaced by a chaotic transient. In a chaotic transient one typically observes orbits which, after being attracted toward the vicinity of the former chaotic attractor, look like what orbits on that chaotic attractor looked like for $p < p_c$. After bouncing around in a chaotic way for a possibly long time such an orbit then, rather suddenly, starts to move off toward some other distant attractor. For example, Fig. 1 shows many iterates of a chaotic transient orbit for the Ikeda map² (a map developed as a model of a laser

ring cavity). The numbers indicate the sequence in which points appear in the figure. Thus after the first few iterations the orbit rapidly approaches the destroyed attractor. The orbit then bounces around on this remnant for about 84435 iterations, after which it "finds its way out," and then rapidly moves off toward an attractor outside the frame of the figure.

The length of a chaotic transient for a particular orbit depends sensitively on the initial condition.¹ However, if one looks at many randomly chosen initial conditions, then one typically sees that τ , the transient lifetime, has an exponential probability distribution, $P(\tau) \approx T^{-1} \exp(-\tau/T)$, for large τ , where T is the mean lifetime of the chaotic transient. In many cases, we find that the dependence of T on the parameter p scales as^{1,3} $T \sim (p - p_c)^{-\gamma}$ for p slightly greater than p_c . We call γ the critical exponent of the chaotic transient. It is the purpose of this paper to develop a theoretical understanding and analytical basis for the prediction of the critical exponent γ for typical situations occurring in two-dimensional maps. (These results will also apply to many three-dimensional continuous-time systems, and we believe that the techniques developed will be useful in other situations, e.g., more dimensions.)

The class of two-dimensional maps addressed in this work are those in which the crisis is due to a tangency of the stable manifold of an unstable periodic orbit with the unstable manifold of another or the same unstable periodic orbit. These types of crises appear to be the *only* kinds of crises which can occur for 2D map systems that are strictly dissipative (i.e., magnitude of Jacobian determinant less than 1 everywhere) and is a ubiquitous feature in such commonly studied nonlinear systems as the forced damped pendulum (or Josephson junction), the forced Duffing equation, the Hénon map (cf. below), and many others. For these systems there is either one of the following two typical types of crises: (i) *Heteroclinic tangency crisis*. In this case, the stable manifold of an unstable periodic orbit (B) on the boundary is tangent to the unstable mani-

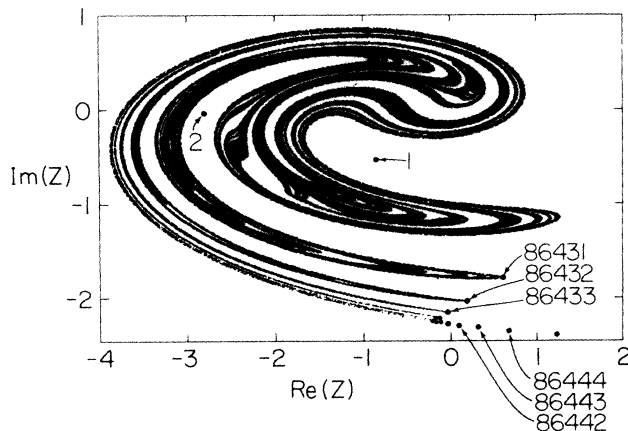


FIG. 1. The Ikeda map is $z_{n+1} = p + Bz_n \exp\{i\kappa - i\alpha/(1 + |z_n|^2)\}$, where z is complex ($z = x + iy$), p is related to the laser input amplitude, B is the coefficient of reflectivity of the partially reflecting mirrors of the cavity, κ is the laser empty cavity detuning, and α measures the detuning due to the presence of a nonlinear medium in the cavity. The parameters are $p = 1.0027$, $B = 0.9$, $\kappa = 0.4$, and $\alpha = 6.0$.

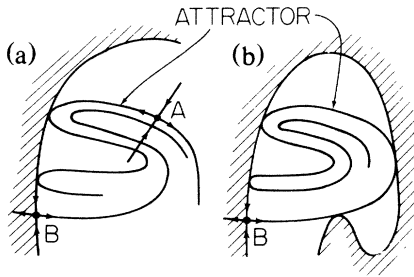


FIG. 2. (a) Schematic illustration of heteroclinic tangencies of the stable manifold of the unstable periodic orbit B and the unstable manifold of the unstable periodic orbit A . (For simplicity we take the periods of A and B to be 1.) Crosshatching denotes the basin of another attractor. (b) Schematic illustration of homoclinic tangencies of the stable and unstable manifolds of the unstable periodic orbit B .

fold of an unstable periodic orbit (A) on the attractor, as in Fig. 2(a). (ii) *Homoclinic tangency crisis*. In this case, the stable and unstable manifolds of an unstable periodic orbit (B) on the boundary are tangent, as in Fig. 2(b).

In both cases, the basin boundary is usually found to be the closure of the stable manifold of the unstable periodic orbit B , as indicated in Fig. 2. The chaotic attractor, on the other hand, is (in both cases) the closure of the branch of the unstable manifold of B that points into the basin. For the case of Fig. 2(a), the chaotic attractor is also the closure of the unstable manifold of A . For both cases, the tangency implies that the chaotic attractor touches the basin boundary (i.e., a crisis⁴).

We argue that the critical exponent γ obeys two distinct laws depending on the type of tangency the system exhibits at the crisis. In the case of a heteroclinic crisis, we have

$$\gamma = \frac{1}{2} + (\ln|\alpha_1|)/|\ln|\alpha_2||, \tag{1}$$

where α_1 and α_2 are the expanding ($|\alpha_1| > 1$) and contracting ($|\alpha_2| < 1$) eigenvalues, respectively, of the periodic orbit A in Fig. 2. In the case of a homoclinic crisis, we have

$$\gamma = (\ln|\beta_2|)/(\ln|\beta_1\beta_2|^2), \tag{2}$$

where β_1 and β_2 are the expanding and contracting eigenvalues of the periodic orbit B in Fig. 2(b). In experiments, a mathematical description of the system is often not available. Nevertheless, the eigenvalues and hence γ can be deduced by an examination of experimental time series at the end of the chaotic transient, and this need only be done for a *single* value of p near p_c . For example, in Fig. 1 the points labeled 86431–86433 are close to the stable manifold of B and are approaching B . Thus they can be used to estimate β_2 . Similarly, points 86442–86444 lie close to the un-

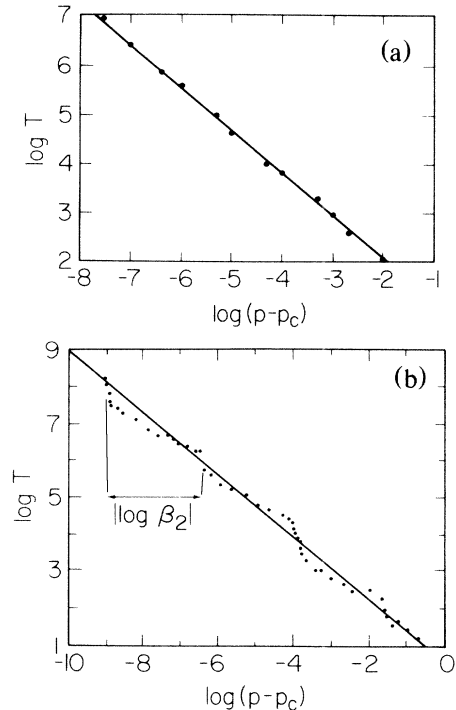


FIG. 3. $\log_{10} T$ vs $\log_{10}(p - p_c)$. Each dot was obtained by an averaging of 300 randomly chosen initial conditions in the former basin of attraction. (a) $J = -0.3$, $p_c = 1.426\,921\,114\dots$; straight line corresponds to γ given by Eq. (1). (b) $J = +0.3$, $p_c = 2.124\,672\,450\dots$, and γ given by Eq. (2).

stable manifold of B and yield an estimate of β_1 .

Figure 3 shows the numerical results (dots) for T vs $p - p_c$ along with the predictions of Eqs. (1) and (2) (the straight lines). The system tested in Fig. 3 is the Hénon map, $x_{n+1} = p - x_n^2 - Jy_n$, $y_{n+1} = x_n$. Figure 3(a) corresponds to a heteroclinic crisis [Eq. (1)], while Fig. 3(b) corresponds to a homoclinic crisis [Eq. (2)]. As is evident from the figures, the agreement with Eqs. (1) and (2) is quite good. Superimposed on the general power-law dependence, Fig. 3(b) also shows evidence of considerable substructure. This is probably due to the striated Cantor set character of the attractor and the fact that the basin boundary is fractal⁵ in this parameter range. As our analysis leading to Eq. (2) shows, the attractor's striations accumulate on the tangency point asymptotically at the geometric rate β_2 . Correspondingly, as indicated in Fig. 3(b), the substructure has a component periodic in $\log(p - p_c)$ with period $|\log\beta_2|$. We proceed now with the derivation of formulas (1) and (2).

Derivation of Eq. (1).—For the heteroclinic crisis, as p is increased past p_c , the unstable manifold of A crosses the stable manifold of B (cf. Fig. 4). An orbit landing in the shaded region ab of the figure is attracted along the stable manifold of B and then rapidly

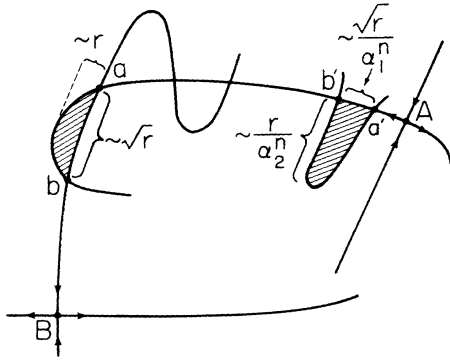


FIG. 4. Schematic diagram illustrating the derivation of Eq. (1).

leaves the transient region moving to the left along the outward branch of the unstable manifold of B . For p near p_c , the dimensions of region ab are of the order⁴ r and $r^{1/2}$, where $r = p - p_c$ (cf. Fig. 4). We now iterate the region ab backwards in time for n steps. For large enough n , except for the first few backwards iterates, the change in the region ab is governed by the linearization of the map about A . Thus the preiterated region $a'b'$ has dimensions of the order of r/α_2^n and $r^{1/2}/\alpha_1^n$, as shown in Fig. 4. Since after falling in region $a'b'$ the orbit soon (i.e., n steps after) falls in region ab , we estimate the transient lifetime as the average time it takes an orbit to land in region $a'b'$. Now consider the probability measure of the attractor at $p = p_c$. T^{-1} is then estimated as the probability that an orbit on the $p = p_c$ attractor falls on a given iterate in the region $a'b'$, and we denote this probability by $\mu(r)$. Now reduce r by the factor α_2 ($r \rightarrow \alpha_2 r$) and consider the resulting region ab . After we iterate backwards $n + 1$ steps (instead of n), the long dimension of the preiterated region is again r/α_2^n but the width is changed to $(\alpha_2 r)^{1/2}/\alpha_1^{n+1}$. Since the attractor is presumed to be smooth in the direction of the unstable manifold of A , we have

$$\frac{\mu(r)}{\mu(\alpha_2 r)} \sim \frac{r^{1/2}/\alpha_1^n}{(\alpha_2 r)^{1/2}/\alpha_1^{n+1}} = \frac{\alpha_1}{\alpha_2^{1/2}}.$$

With the assumption that $\mu(r) \sim r^\gamma$, Eq. (1) then follows.

Derivation of Eq. (2).—Refer to Fig. 5 which corresponds to the case $p = p_c$. Let y be the distance from B along the upper segment of the stable manifold of B , and let x denote the distance from B along the right-going segment of the unstable manifold of B . In the figure we have drawn these manifolds as being perpendicular straight lines near B , and we shall treat the distances x and y as Cartesian coordinates (this can be accomplished via a change of variables). A tangency occurs at $(x, y) = (0, y_0)$. Consider the cross-hatched region ab indicated in the figure, where the right-hand

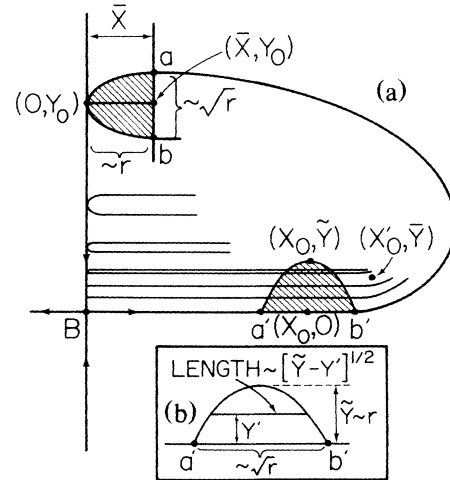


FIG. 5. (a) Schematic diagram illustrating the derivation of Eq. (2). (b) Blowup of region $a'b'$.

boundary of this region is the vertical line $x = \bar{x}$. We estimate T^{-1} at $r = p - p_c \ll 1$ as the measure $\mu(r)$ of the attractor in the shaded region ab for $\bar{x} \cong Kr$ (where K is a constant), i.e., $T^{-1} \sim \mu(r)$. Say that the point $(x_0, 0)$ is the first backward iterate of the tangency point $(0, y_0)$, that region $a'b'$ is the first backward iterate of region ab , and that the point (\bar{x}, y_0) maps to (x'_0, \bar{y}) after n forward iterations, where n is the smallest integer such that $x'_0 > x_0$. For small \bar{x} , most of the n iterations mapping (\bar{x}, y_0) to (x'_0, \bar{y}) occur near B , where the map is nearly linear.⁶ Thus $\bar{x}\beta_1^n \sim x'_0$ and $\bar{y}\beta_2^n \sim y_0$, which yields $\bar{x} \sim (\bar{y})^\rho$ with $\rho = (\ln\beta_1)/|\ln\beta_2|$. As indicated in Fig. 5, the part of the attractor near $(x_0, 0)$ is striated into bands running nearly parallel to the unstable manifold of B and has a smooth structure along these bands. At $x = x'_0$ let $\psi(\bar{y})d\bar{y}$ denote the measure of the attractor per unit length in x between \bar{y} and $\bar{y} + d\bar{y}$. [Strictly speaking, the probability density $\psi(\bar{y})$ does not in general exist, but we shall talk as if densities do exist.] As a result of the assumed smoothness of the attractor probability measure parallel to the unstable manifold, $\psi(\bar{y})$ evaluated at x'_0 and at x_0 are of the same order. Let $\phi(\bar{x})$ be the ‘‘probability density’’ $\phi(\bar{x}) = d\mu/d\bar{x}$. By conservation of probability we now obtain two relationships between $\phi(\bar{x})$ and $\psi(\bar{y})$. First since (\bar{x}, y_0) maps to (x'_0, \bar{y}) in n iteration, we have $\phi(\bar{x})d\bar{x} \sim \psi(\bar{y})d\bar{y}$; and, using $\bar{x} \sim (\bar{y})^\rho$, we have our first relationship, $\psi(\bar{y}) \sim (\bar{y})^{\rho-1}\phi(\bar{y}^\rho)$. The second will be the result of the fact that region $a'b'$ maps on one iteration to region ab . Hence the two regions have the same measure. Region $a'b'$ has measure $\mu \sim \int_0^{\bar{y}} \psi(y')(\bar{y} - y')^{1/2} [cf. Fig. 5(b)]$. Since (x_0, \bar{y}) maps to (\bar{x}, y_0) on one iteration we set $\bar{y} \approx K\bar{x}$ for small \bar{x} and \bar{y} . Hence,

$$\phi(\bar{x}) = d\mu/d\bar{x} \sim \int_0^{K\bar{x}} \psi(y')(K\bar{x} - y')^{1/2} dy'.$$

This is our second relationship between ϕ and ψ . Assumption of a power-law dependence of ϕ on \bar{x} , viz. $\phi(\bar{x}) \sim (\bar{x})^\alpha$, and substitution into our two relationships between ϕ and ψ , yields $\alpha = (\rho - 1/2)/(1 - \rho)$. Now utilizing $\mu = \int_0^{\bar{x}} \phi(x') dx'$, we have $T^{-1} \sim \mu \sim (\bar{x})^{\alpha+1} \sim r^{(\alpha+1)}$, or $\gamma = \alpha + 1 = [2(1 - \rho)]^{-1}$, which is Eq. (2), the desired result.

In all the preceding discussions we have been concerned with crises which *destroy* the attractor, replacing it with a chaotic transient. We note that there are other types of crises,¹ called interior crises, in which a sudden increase of the phase-space extent of the attractor (rather than destruction of the attractor) takes place.¹ Before the interior crisis, a dynamical variable (call it x) would vary chaotically but always be restricted to some region (say $x_2 > x > x_1$), or a finite number of such regions. (The latter is the case for the period-three interior crisis discussed in Ref. 1.) Slightly after the interior crisis, the time behavior would be highly intermittent: x would usually lie in the region to which it was formerly restricted, but occasionally it would, rather suddenly, burst out of the restricted region, bounce around far outside it, and then return to the former restricted region. Critical behavior near the interior crisis could, for example, be characterized by the average time between bursts. This should scale with $|p - p_c|^{-\gamma}$ with γ given by the *same formulas* as for chaotic transients [viz., Eqs. (1) and (2)]. Scaling for interior crises may be more accessible experimentally than is the scaling of chaotic transients, because many initial conditions are necessary to obtain the average transient lifetime, whereas the average time between bursts is obtainable from a single orbit.

Finally, we note that in practice the experimental observability of chaotic transients (for boundary crises) and intermittent bursts (for interior crises) depends strongly on the size of the exponent. For example, for one-dimensional maps with a quadratic maximum, $\gamma = \frac{1}{2}$, which implies⁷ that to see transients longer than ~ 100 requires p to be within the order of 0.01% of p_c ! On the other hand, if $\gamma \sim 2$ (as is the case of the map in Fig. 1) then transients longer than 100 might be expected to exist over a range of p of the

order of 10%, a much more favorable situation for experimental measurement. We believe that the fact that γ tends to be larger for two-dimensional maps as compared to one-dimensional maps indicates a general trend in that transients associated with more-dimensional attractors should be more persistent. Indeed, it has been a puzzle as to why chaotic transients and chaotic bursts are so persistent with respect to parameter variation in some experiments⁸ and numerical computations⁹ on more-dimensional systems.

This work was supported by the U.S. Department of Energy, Office of Basic Energy Sciences (Applied Mathematics Program).

^(a)Laboratory for Plasma and Fusion Energy Studies.

^(b)Departments of Electrical Engineering and of Physics.

^(c)Institute for Physical Science and Technology and Department Mathematics.

¹C. Grebogi, E. Ott, and J. A. Yorke, *Physica* (Amsterdam) **7D**, 181 (1983), and *Phys. Rev. Lett.* **48**, 1507 (1982).

²K. Ikeda, *Opt. Commun.* **30**, 257 (1979).

³Another type of scaling which yields superpersistent chaotic transients has been investigated by C. Grebogi, E. Ott, and J. A. Yorke, *Phys. Rev. Lett.* **50**, 935 (1983), and *Ergodic Theory Dynamical Systems* **5**, 341 (1985).

⁴From here on we consider only the generic case in which the tangency is nondegenerate, that is, the contact is second order.

⁵S. W. McDonald, C. Grebogi, E. Ott, and J. A. Yorke, *Physica* (Amsterdam) **17D**, 125 (1985); C. Grebogi, S. W. McDonald, E. Ott, and J. A. Yorke, *Phys. Lett.* **99A**, 415 (1983).

⁶Indeed, in general, there exists a smooth change of variables, for which the map is linear in a finite neighborhood of B [P. Hartman, *Ordinary Differential Equations* (Wiley, New York, 1964)].

⁷We assume here that, for a physically reasonable definition and normalization of the parameter p , the constant κ in the formula $T \approx \kappa [(p - p_c)/p_c]^{-\gamma}$ is of order unity (cf., for example, Fig. 3).

⁸P. Bergé and M. Dubois, *Phys. Lett.* **93A**, 365 (1983).

⁹J. M. Hyman, B. Nicolaenko, and S. Zaleski, Los Alamos National Laboratory Report No. LA-UR-86-1947, 1986 (to be published).